PHILOSOPHICAL TRANSACTIONS OF THE ROYAL SOCIETY A MATHEMATICAL, PHYSICAL & ENGINEERING SCIENCES

Short-Range Order in Crystals of Anthrone and in Mixed Crystals of Anthrone-Anthraquinone

H. D. Flack

Phil. Trans. R. Soc. Lond. A 1970 **266**, 583-591
doi: 10.1098/rsta.1970.0014

III. SHORT-RANGE ORDER IN CRYSTALS OF ANTHRONE AND IN MIXED CRYSTALS OF ANTHRONE–ANTHRAQUINONE

By H. D. FLACK

[Plates 10 and 11]

CONTENTS

Stationary crystal photographs of anthrone taken with white + CuK radiation and with [010] normal to the incident beam show diffuse intermediate layer lines corresponding with $k = \frac{1}{2}, \frac{3}{2}$, etc. A pseudo-Weissenberg technique has been developed for the study of the $h\frac{1}{2}l$, etc. layers which gives good resolution of these diffuse scattering regions. Measurement of the integral breadth of these scattering maxima show that there are, in anthrone, short-range-order domains of average length 9 molecules (36 Å) in the [010] direction and 3 molecules (25 Å) in the [001] direction, the arrangement along [100] being random. In mixed crystals, up to 12 mole per cent of anthraquinone can crystallize with anthrone without disturbing this short-range order. At the other extreme of the phase diagram, no short-range order is found for up to 45 mole % anthrone in anthraquinone. The region 12 to 55 mole % of anthraquinone in anthrone seems to define a miscibility gap; no crystals of these compositions could be made.

Introduction: experimental technique

The aim of part II was to obtain mathematical relations connecting the X-ray diffraction patterns given by a crystal containing regions of short-range order with the dimensions of those regions.

The pattern of scattering from such a crystal consists of the usual, relatively sharp diffracted beams together with diffuse beams of considerable extent. These are best sampled or studied by using a stationary crystal and an incident beam containing both continuous and characteristic wavelengths, thus obtaining a Laue pattern with a diffuse background pattern, the latter being given by the characteristic component. A series of such patterns effectively investigates reciprocal space by means of *spherical* sections. Such sections enable the shapes and extents of the diffuse scattering regions to be determined more surely than by any other technique. Photographic techniques combined with isodensitracer intensity measurements (Milledge 1969) give both a permanent record and accurate data, the main advantage of photography being that the shapes and scattering density of large regions of diffuse scattering having no sharp outline can be

determined at any given period of time, and under any given conditions of temperature and pressure, all of one section being recorded simultaneously on the photograph, although different areas of the section are measured consecutively by the isodensitracer.

This *systematic* exploration of reciprocal space by means of stationary crystal photographs taken with white plus characteristic radiation was first demonstrated by Lonsdale, Knaggs & Smith (1940), Lonsdale & Smith (1941) and Lonsdale (1942), who showed that there could exist two kinds of diffuse scattering: (1) the thermal diffuse scattering which was markedly temperature-sensitive, (2) diffuse scattering due to static disorder (in diamonds) the intensity of which was temperature-independent or almost so. More recently, Amorós & Amorós (1968) have made an extensive study of the transforms and diffuse scattering of molecular crystals using this method of 'systematic Laue photographs'.

Hoppe (1964) has used the same method, but has also taken equi-inclination Weissenberg photographs recording layers of reciprocal space between the reciprocal lattice planes. This method has the advantage of recording the whole of the diffuse scattering, for any particular non-integral index, on one photograph but it has the disadvantage of requiring long exposure times, even for crystals larger than those normally best suited to crystal structure analysis; and of course the resolution is not good. Precession photographs may also be used to record the diffuse scattering, but their range is limited.

Diffractometer techniques are not suited to this type of investigation except in certain very limited circumstances. Their disadvantages are: (1) lack of resolution when the diffuse scattering regions are of large extent, and (2) the fact that recordings are made consecutively in time; so that conditions may change during the course of the observations, especially if the crystal itself is volatile or subject to chemical or textural change when irradiated or allowed to age.

The diffuse scattering of anthrone

Crystals of anthrone grown from diethyl ether, ethanol or acetic acid all gave the diffuse scattering of Cu Kα radiation first observed on rotation photographs by Banerjee & Srivastava (1960) and attributed by them to disorder. This consists of layer-lines of diffuse spots at $k = \frac{1}{2}$ and $\frac{3}{2}$, observable on oscillation or rotation photographs about [010] but more easily on stationary-crystal patterns using white and characteristic radiation, [010] being along the axis of the cylindrical film and therefore normal to the incident X-ray beam. Figure 1, plate 10, shows a typical stationary-crystal photograph, taken at 20 °C. It clearly shows two types of diffuse spot. The one type (which is the ordinary thermal scattering) is always associated with some neighbouring Laue spot which lies nearly or exactly along a radial direction through the diffuse spot. The other diffuse spots, which lie along the $k = \frac{1}{2}, \frac{3}{2}$ layer-lines, are not associated with any identifiable Laue spots, and also obey a different law of temperature variation. Figure 2, plate 10, which is a stationary-crystal photograph of the isostructural anthraquinone, in an orientation similar to that of figure 1, shows only the thermal diffuse spots and not the intermediate layer-line type. Figure 3, plate 10, shows a pair of anthrone stationary-crystal patterns, taken at 20 and -170° C respectively. The thermal diffuse spots decrease in intensity as the temperature decreases. The intermediate layer-line diffuse spots *increase* in intensity as the temperature decreases, especially at higher angles of scattering. The thermal diffuse scattering is due to dynamic disorder, the diffuse scattering which occurs at $k = \frac{1}{2}$ and $\frac{3}{2}$ is of the kind discussed in part II of this paper; it is due to static short-range order in a long-range disordered pseudo-symmetric crystal. The symmetry of both types of diffuse scattering is $2/m$.

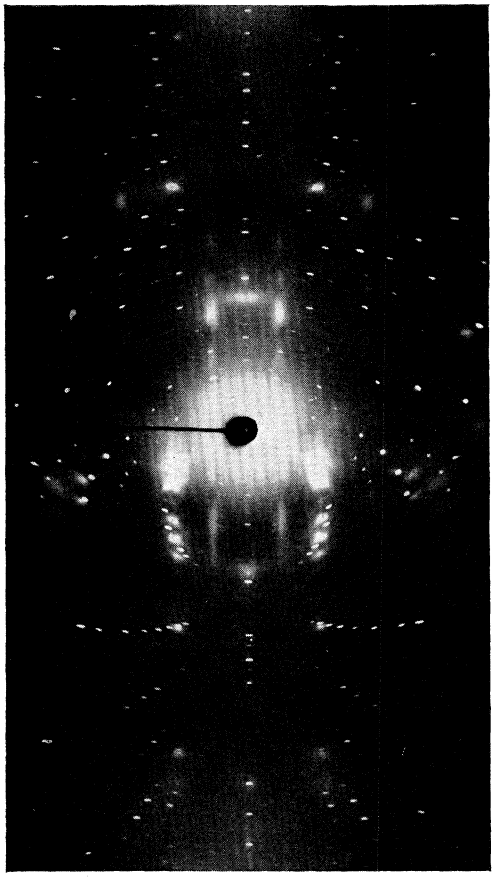

FIGURE 1. Typical stationary-crystal photograph of anthrone, 20 °C, showing two types of diffuse spot: [010] vertical, white + Cu K radiations. ([010] left-to-right in figures 1 to 3).

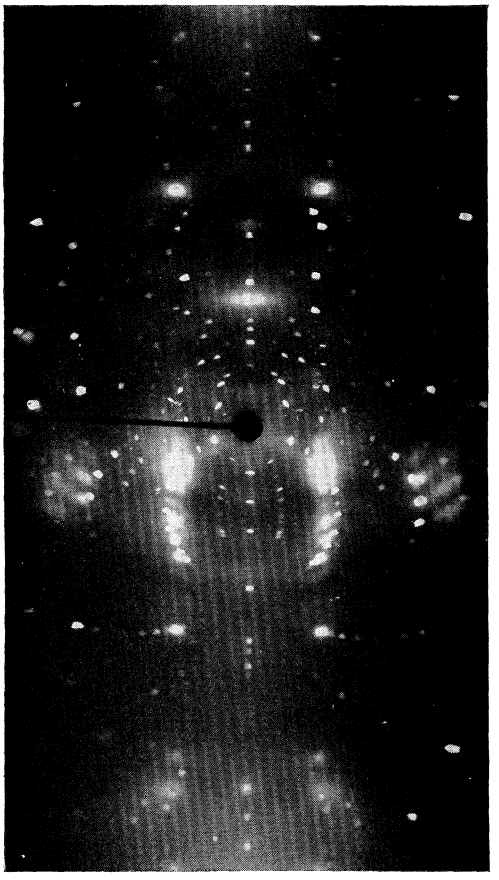

FIGURE 2. Stationary-crystal photograph of anthraquinone, in a setting near to that of the isostructural anthrone (figure 1). No 'disorder' spots.

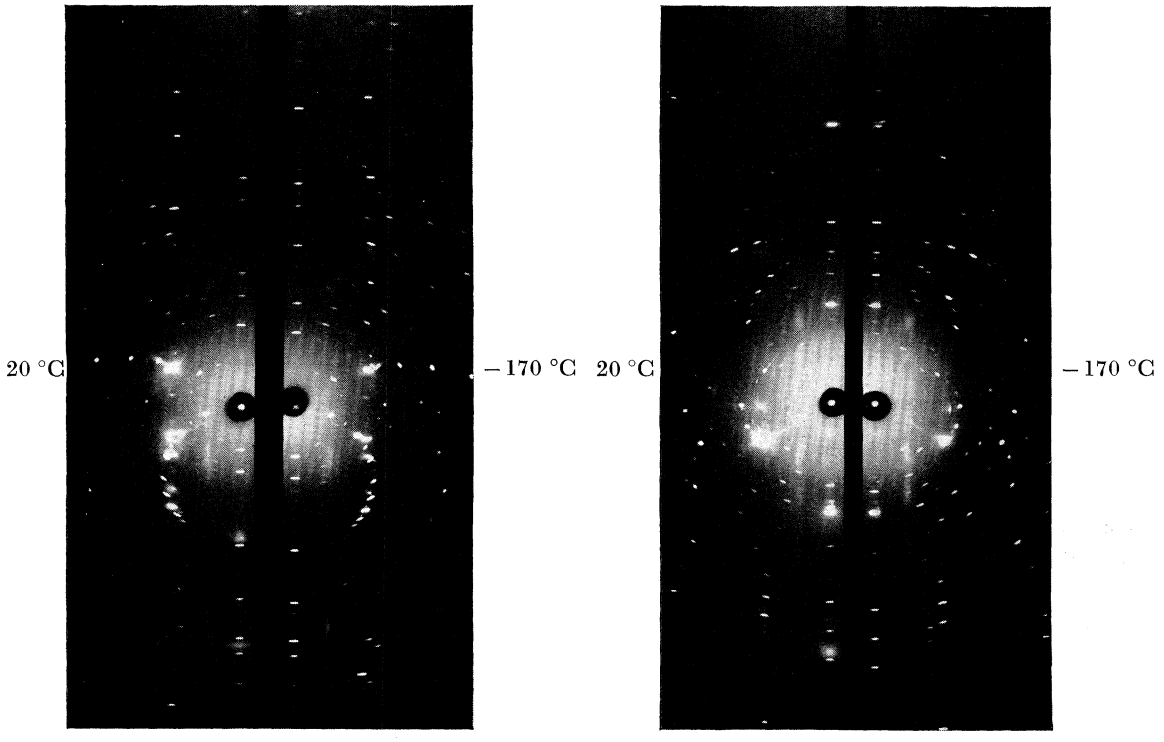

FIGURE 3. A pair of similar anthrone photographs taken at 20 °C (left), and −170 °C (right) respectively Two different settings. The thermal diffuse scattering is weakened at low temperatures, whereas most Laue spots and the 'disorder' diffuse scattering are relatively more intense.

(*Facing p.* 584)

PHILOSOPHICAL TRANSACTIONS OF THE ROYAL SOCIETY A MATHEMATICAL, PHYSICAL & ENGINEERING SCIENCES

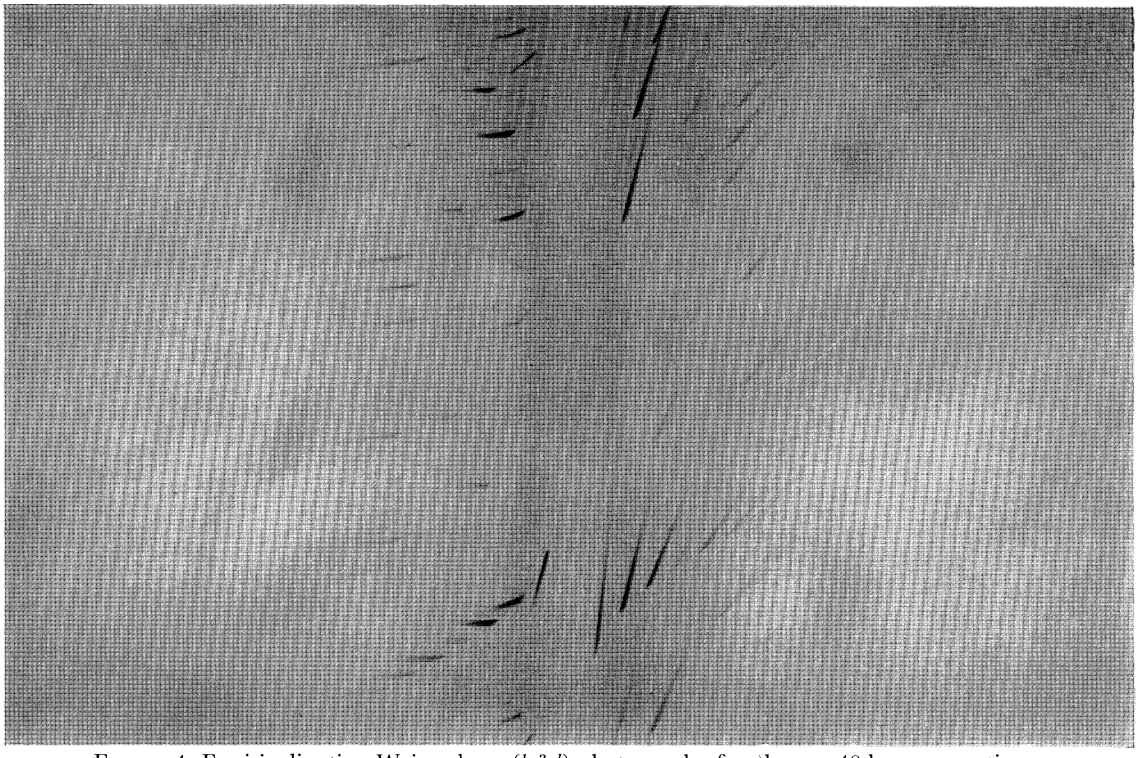

FIGURE 4. Equi-inclination Weissenberg $\{h\,\frac{3}{2}\,l\}$ photograph of anthrone, 48 h exposure time, filtered Cu Kα radiation, 5.73 cm diameter Nonius camera. Note comparative lack of detail.

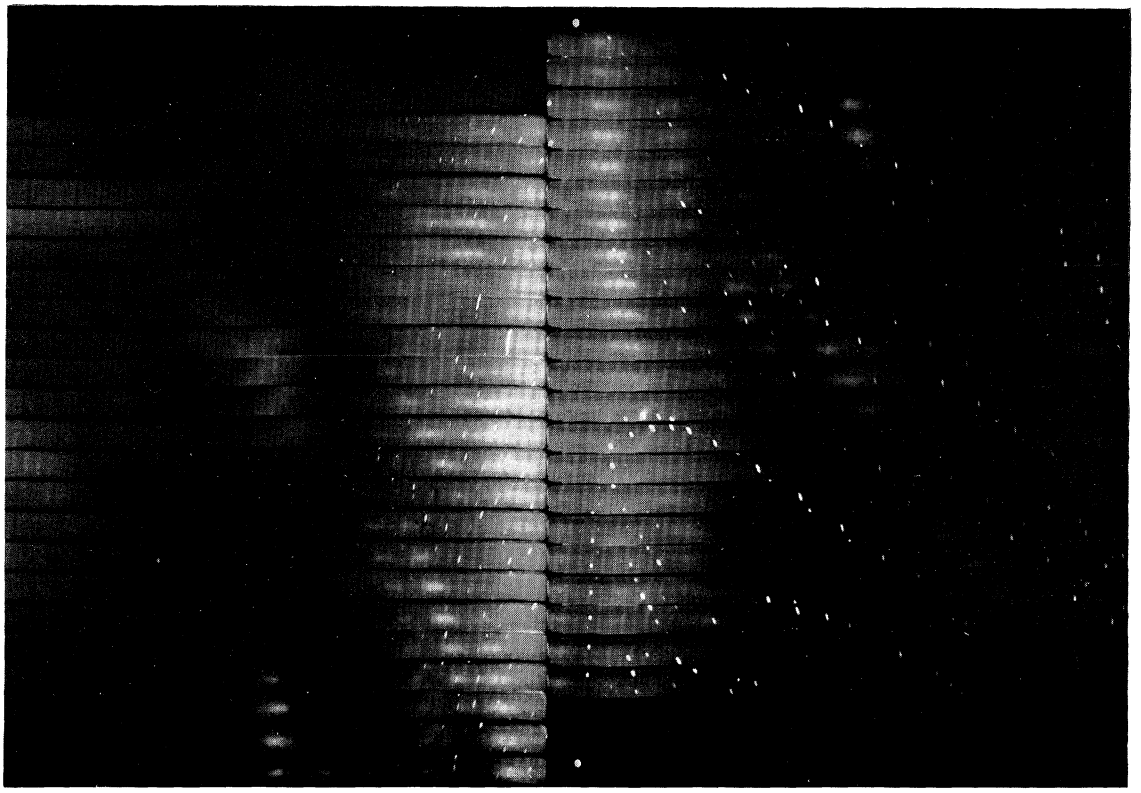

FIGURE 5. One set of $\{h\,\frac{1}{2}\,l\}$ (left) and $\{h\,\frac{3}{2}\,l\}$ (right) stationary-crystal strip photographs taken on a Weissenberg camera set for equi-inclination $\{h\,1\,l\}$. Each of the 22 crystal orientations was given 2 h exposure time before resetting the crystal by 5° at a time and moving the camera forward by a corresponding 2.5 mm. Note the increased intensity and resolution as compared with figure 4. (Figure 5 is at right angles to figures 1, 3, plate 10.)

PHILOSOPHICAL TRANSACTIONS OF THE ROYAL SOCIETY A MATHEMATICAL, PHYSICAL & ENGINEERING SCIENCES

The problems are now to obtain the clearest record of the short-range order diffuse scattering and to interpret it quantitatively.

(*a*) *Systematic recording of the diffuse scattering of anthrone*

Equi-inclination Weissenberg photographs of the $\{h\,\frac{1}{2}\,l\}$ and $\{h\,\frac{3}{2}\,l\}$ layers were taken by mounting a crystal parallel to [010], and using a 5.73 cm diameter Nonius camera with filtered Cu Kα radiation and a 48 h exposure time (30 kV, 24 mA). As figure 4, plate 11, shows, the detail was poor, and it was decided that this lack of resolution was intrinsic and little improvement could be expected even with a longer exposure time using monochromatized radiation.

The detail and clarity of the diffuse layer recorded on stationary-crystal patterns (as in figure 1) indicated that some modification of the 'systematic Laue' method would be the most suitable for purposes of observation and measurement. The equi-inclination Weissenberg camera was used, with specially designed layer-line screens made to allow the simultaneous recording, on different parts of the film, of the $h\,\frac{1}{2}\,l$ and $h\,\frac{3}{2}\,l$ diffuse reflexions. Then instead of a smooth rotation or oscillation of the crystal synchronized with a translatory movement of the film behind the screens, a series of consecutive stationary-crystal photographs was taken, with the film moved forward by steps corresponding with the width of the screen gap and the angular separation (5°) of the consecutive crystal positions. The inclination angle used was that for equi-inclination of the $h\,1\,l$ layer and each orientation of the crystal was given an exposure time of 2 h. Stabilized, unfiltered Cu K radiation was used. It was possible to record 22 exposures on any one film; thus the 36 exposures necessary to cover 180° by 5° steps could be accommodated on two films, with

FIGURE 6. Isodensitracer record of part of the film shown in figure 5, plate 11. The part shown is the bottom five strips of $\{h\,\frac{1}{2}\,l\}$. Optical wedge varies in optical density from 0 to 3.

some additional identical records for purposes of correlation. Figure 5, plate 11, shows one such film.

(*b*) *Measurement of intensity and shape of the diffuse scattering*

The Joyce–Loebl Isodensitracer (Milledge 1969; Milledge & Graeme-Barber 1969) is ideal for measurement of the diffuse-scattering regions. One of the photometric records, obtained by using a magnification of 10 and an optical wedge varying in optical density from 0 to 3, is shown in figure 6.

The steps required to interpret the I.d.t. photometric record in terms of the geometry and intensity of diffuse scattering in reciprocal space are fully described by Flack (1968). Briefly, they are as follows:

(i) Construction of contour plots of the non-equi-inclination pseudo-Weissenberg photographs of $\{h\frac{1}{2}l\}$ and $\{h\frac{3}{2}l\}$.

(ii) Conversion of these contour plots to reciprocal space. This was done by means of facilities provided in the intensity processing program of Milledge & Milledge (1961), Milledge (1962).

(iii) Application of suitable intensity correction factors. Although the latter might alter the magnitude of the relative intensities of the diffuse maxima, they would not affect their positions. In order to compare observed and calculated diffuse scattering only general agreement between the uncorrected distribution of observed diffuse scattering and the calculated $\overline{F^2}$ distribution was attempted.

The experimentally-determined intensity distributions for the $\{h\frac{1}{2}l\}$ and $\{h\frac{3}{2}l\}$ sections of reciprocal space are shown in figures 7*a* and 8*a* respectively.

(*c*) *Calculation of the diffuse scattering and hence the average dimensions of blocks of short-range order in anthrone*

The values of $\overline{F^2}$ for the theoretical 'disorder' diffuse scattering are given by equation (14) in part II,

$$\overline{F^2}\,(\text{diffuse}) = \tfrac{1}{4}\{|G_0 - G_0'|^2 + |G_1 - G_1'|^2\}\, y_a y_b y_c,$$

where y_a, y_b, y_c are functions of the probabilities α, β, γ of a 'mistake' of orientation of the molecule along ***a***, ***b***, ***c*** respectively.

The transforms $\overline{F^2}$ should really be continuous, but for purposes of computation a unit of $0.04\,\text{Å}^{-1}$ in reciprocal space was used, and the maximum value of 0.47 was taken for $(\sin\theta)/\lambda$ since no measurable diffuse scattering was observed beyond this value. All the atomic positional and thermal parameters required for the calculation were taken from the results of the crystal structure analysis given in part I.

The case of two non-centrosymmetric molecules of a single chemical species in the statistical space group $P2_1/a$, considered in part II, applies to anthrone with the additional simplification that the anthracene skeleton of the molecule is, for practical purposes, centrosymmetric. For these 14 carbon and 8 hydrogen atoms $G_0 = G_0'$ and $G_1 = G_1'$; so that in the computation of $|G_0 - G_0'|^2$ and $|G_1 - G_1'|^2$ only the one oxygen and two hydrogen atoms H 13 and H 14 need be taken into account.

Since rotating- and stationary-crystal photographs of anthrone both show intermediate diffuse [010] layer lines, it follows (see part II) that $\beta > 0.5$ and from equation (16) of part II, the value of β can be estimated from the integral breadth w of the diffuse profile. A technique for measuring w for a diffuse maximum had to be devised. Individual graphs of intensity parallel to [010] passing through the centre of a diffuse maximum in $h\frac{1}{2}l$ were constructed from the isodensitracer records shown in figure 6, first against a film coordinate y (mm) parallel to the rotation axis

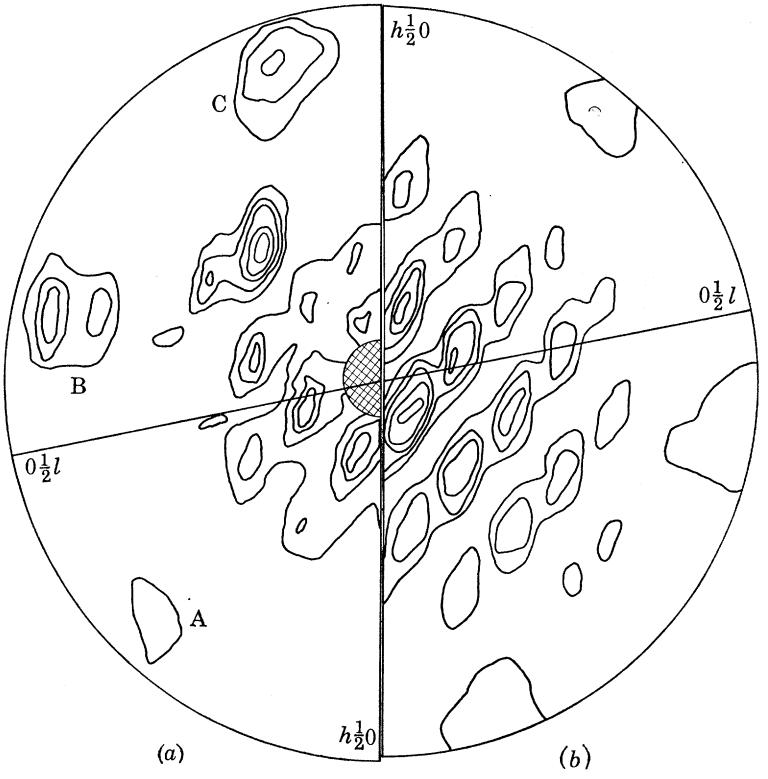

FIGURE 7. Distribution of diffuse scattering in the $\{h\,\frac{1}{2}\,l\}$ section of reciprocal space appropriate to Cu Kα radiation: (*a*) as experimentally observed, (*b*) as calculated for $\alpha = 0.5$, $\beta = 0.89$, $\gamma = 0.68$ for the disorder diffuse scattering, and with the difference Fourier transform superimposed to give the thermal scattering effect also.

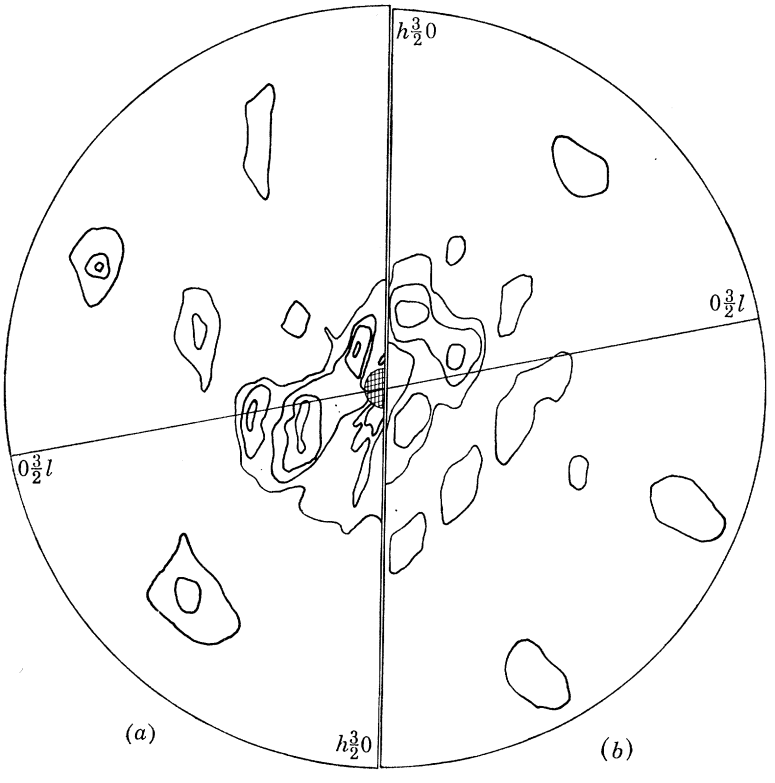

FIGURE 8. As figure 7, for the $\{h\,\frac{3}{2}\,l\}$ section.

[010] and thence against $K\ (=2\pi\zeta(b/\lambda))$. (See *International tables for X-ray crystallography*, **2**, 175.) Figure 9 shows this process for one typical maximum. The peak height of each diffuse maximum (at $K=\pi$) could be measured; and integrated intensities were compared by cutting out from the graph paper the shapes of the profiles and weighing them, the weight of a known area of the graph paper being known. Hence the integral breadths of the maxima could be determined. From three values of w parallel to [010] β was found to be 0.89 ± 0.02.

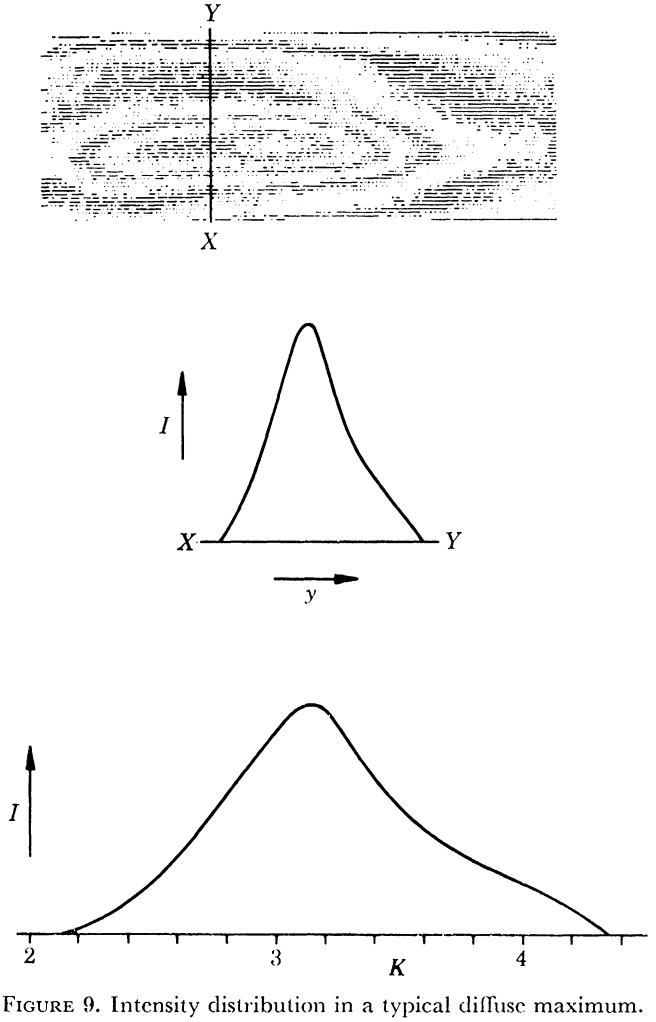

FIGURE 9. Intensity distribution in a typical diffuse maximum.

The 'observed' patterns shown in figures 7*a* and 8*a* indicate that there exists some layering of spots normal to [001] (at $l=\frac{1}{2},\frac{3}{2},\frac{5}{2}$, etc.) but not normal to [100]. This implies a value of $\gamma>0.5$. Parallel to [100] there is complete disorder, giving $\alpha=0.5$.

For three 'disorder' diffuse maxima in the $h\frac{1}{2}l$ section, as observed and then plotted in reciprocal space, a measurement of intensity along [001] was plotted against L; and hence a value of $\gamma=0.68\pm0.02$ was deduced.

The figures 7*a* and 8*a* must also contain the thermal diffuse scattering and for purposes of calculation this may be obtained from the difference Fourier transform (d.F.t.) $\Sigma(F_0^2-F_t^2)$ where F_0 is the Fourier transform of the molecule at rest and F_t is that at temperature t, the summation being taken over both molecules in the unit cell. In making the calculation, the oxygen atom

and the two hydrogen atoms H 13 and H 14 were given site-occupation values of 0.5. The *separate* calculated data for $h\frac{1}{2}l$ for $\alpha = \gamma = 0.5$, $\beta = 0.89$, for $\alpha = 0.5$, $\beta = 0.89$, $\gamma = 0.68$ and for the d.F.t. are shown in figure 10*a*, *b*, *c* respectively.

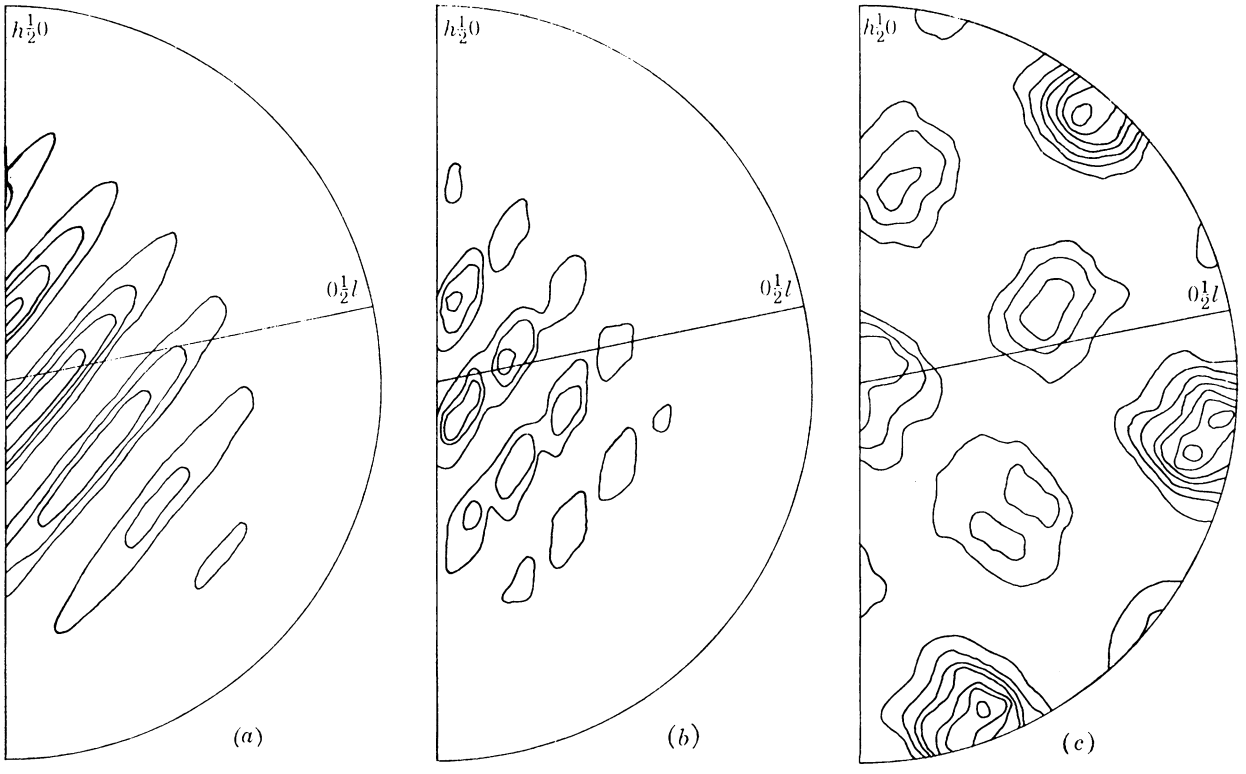

FIGURE 10. Calculated diffuse scattering for $\{h\frac{1}{2}l\}$: (*a*) for 'disorder' only, based on $\alpha = \gamma = 0.5$, $\beta = 0.89$; (*b*) for 'disorder' only, based on $\alpha = 0.5$, $\beta = 0.89$, $\gamma = 0.68$; (*c*) for difference Fourier transform only. (Note that figure 7*b* shows the sum of 10*b* and *c* together.)

The total diffuse scattering arising from disorder corresponding with $\alpha = 0.5$, $\beta = 0.89$, $\gamma = 0.68$ and from the thermal scattering given by the d.F.t. (both being on the same absolute intensity scale) was calculated for $h\frac{1}{2}l$ and $h\frac{3}{2}l$ and the results are shown in figures 7*b* and 8*b* for comparison with the observed data.

The agreement is good, for these two sections, between the observed and calculated diffuse scattering patterns. The values obtained for α, β, γ may therefore be used to calculate the average lengths of short-range order $a/2(1-\alpha)$,† $b/(1-\beta)$, $c/(1-\gamma)$ along the [100], [010] and [001] directions. These are respectively 16 ± 1 Å, 36 ± 9 Å and 25 ± 2 Å, corresponding with:

(i) A random choice between ... R R ... W W ... W R ... and ... R W ... along [100].

(ii) A short-range order ... R W R W ... for an average of $9(\pm 2)$ of molecules along [010].

(iii) The same for an average of $3.1(\pm 0.4)$ molecules along [001].

The effect is one that could correspond with small areas of checker-board short-range order parallel to (100), each a little larger, on average, than 9 molecules (along *b*) by 3 molecules (along *c*), or having an overall area of $9(\pm 2) \times 10^2$ Å^2, but with random ordering in a direction normal to (100).

† $a/2(1-\alpha)$ because there are two molecules along [100] in each unit cell.

Mixed crystals of anthrone–anthraquinone

The close similarity between the molecular and crystal structures of anthrone and anthraquinone shown in part I suggests that they may form a mixed-crystal series. Anthraquinone has an ordered structure and the solution of anthrone in anthraquinone must produce initial disorder. Anthrone is disordered, with regions of short-range order. It is of interest to see whether the introduction of anthraquinone molecules breaks up these regions or whether at first the short-range ordered regions remain intact, the anthraquinone molecules going between them.

Harris (1965) prepared mixed crystals by melting anthrone and anthraquinone together in known proportions in a sealed tube and allowing the mixture to cool slowly in a vacuum flask. Acicular crystals were formed which were usually distorted and which were assumed to have the composition of the mixture put into and sealed in the tube. Any variation from this composition must have resulted in a mixture of two or more different compositions.

An attempt to obtain undistorted crystals was made by crystallization from solvents. However, anthraquinone is much less soluble than anthrone and always crystallizes out first unless the solutions used are saturated with respect to both primary components. It was found that mixed crystals could be grown from a warm methyl ethyl ketone solution which contained over 90 mole % of anthrone with variable amounts of anthraquinone, and which was allowed to cool slowly. Their composition could not be determined with certainty from u.v. or i.r. absorption spectra. Density or melting-point measurements would be effective if reliable calibration curves were available, but this was not the case; although either would give a rough answer. Chemical analysis and n.m.r. spectroscopy would have required more material than was available. What was wanted was a non-destructive method applicable to very small single crystals and this was available in the study of X-ray diffraction intensities, using the formula

$$F^2_{\text{calc}} = (1/S)[xF_Q + (1-x)\,F_N]^2,$$

where S is a scaling factor ($\Sigma F^2_{\text{obs}}/\Sigma F^2_{\text{calc}}$), x is the mole fraction of anthraquinone (Q) in the mixed crystal and $(1-x)$ is the mole fraction of anthrone (N). If the crystal were twinned (as frequently occurred) a modification of this formula had to be used. Table 1 gives the $h\,0\,l$ reflexions used and their values of F_Q and F_N.

Table 1. F_{calc} for various $h\,0\,l$ reflexions, as given in El Sayed (1965) and in table 2 of part I of this paper (pp. 563–567)

$h\,0\,l$	anthraquinone (F_Q)	anthrone (F_N)
002	−15.12	−9.60
400	−16.08	−11.27
004	−9.08	−10.89
800	−6.44	−9.93
204	−13.22	−12.72
801	−15.98	−13.83
203	−19.52	−15.97
601	−20.04	−15.65
202	9.20	8.37
401	7.44	7.69
201	−3.80	−9.33

A standard least-squares procedure was used to determine the best values of S and x from the $\{h\,0\,l\}$ experimental data for any given crystal; $\{h\,1\,l\}$ photographs were used too.

It was found that the mixed crystals could be divided roughly into three composition ranges, within any one of which the properties were generally very similar.

x = 0 to 12 mole per cent of anthraquinone

The crystals within this range have the same morphology as anthrone, being good single crystals, acicular along [010], with side faces {100}, {001} and {20$\bar{1}$}. Stationary-crystal X-ray photographs showed diffuse layers similar in integral breadth and arrangement to those obtained for pure anthrone, although qualitatively there appeared to be a general weakening of 'disorder' diffuse intensity as the proportion of anthraquinone increased. The implication is that the regions of short-range order of anthrone remain of the same size, although they are diluted by the presence of anthraquinone which, however, does not penetrate them and which is not regularly arranged in any way.

x = 12 to 55 mole per cent anthraquinone

Despite repeated attempts, no mixed crystals within this composition range were ever made. This suggests that there is a miscibility gap in the anthrone, anthraquinone phase diagram (compare Glazer (1968) and this series, part VI).

x = 55 to 100 mole per cent anthraquinone

The crystals in this range appeared to be more plate-like than in the 0 to 12 % range, and many of them were twinned on (20$\bar{1}$). All were either cracked or distorted, and none of the $k = \frac{1}{2}(2n+1)$ diffuse scattering was found for any crystal in this range. It appears, therefore, that there is a random distribution of anthrone and anthraquinone molecules over the lattice sites.

References

Amorós, J. L. & Amorós, M. 1968 *Molecular crystals: their transforms and diffuse scattering*. New York: Wiley.
Banerjee, K. & Srivastava, S. N. 1960 *Indian J. Phys.* **34**, 184.
El Sayed, K. 1965 Thesis, London.
Flack, H. D. 1968 Thesis, London.
Glazer, A. M. 1968 Thesis, London.
Harris, J. W. 1965 *Nature, Lond.* **206**, 1038.
Hoppe, W. 1964 *Advances in structure research by diffraction methods*, p. 90. Braunschweig: Vieweg.
Lonsdale, K. 1942 *Rep. Prog. Phys.* **9**, 256.
Lonsdale, K., Knaggs, I. E. & Smith, H. 1940 *Nature, Lond.* **146**, 332.
Lonsdale, K. & Smith, H. 1941 *Nature, Lond.* **148**, 112.
Milledge, H. J. 1962 *Proc. Roy. Soc. Lond.* A **267**, 566.
Milledge, H. J. 1969 *Acta crystallogr.* A **25**, 173.
Milledge, H. J. & Graeme-Barber, A. 1969 *Joyce–Loebl Rev.* **2**, 2.
Milledge, H. J. & Milledge, D. 1961 *Computing methods and the phase problem in X-ray crystal analysis*, p. 79. Oxford: Pergamon.

PHILOSOPHICAL TRANSACTIONS OF THE ROYAL SOCIETY A MATHEMATICAL, PHYSICAL & ENGINEERING SCIENCES

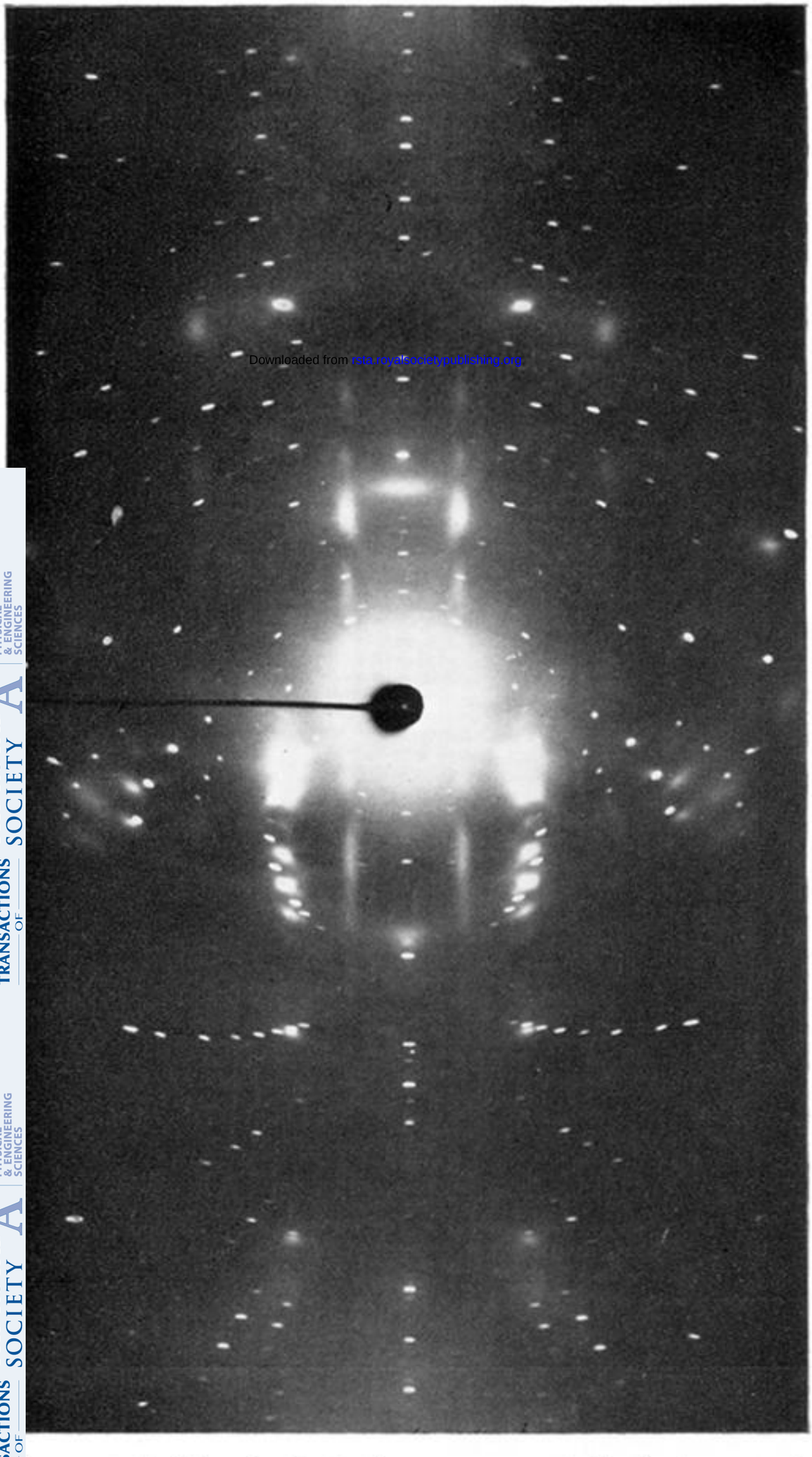

PHILOSOPHICAL TRANSACTIONS OF THE ROYAL SOCIETY A MATHEMATICAL, PHYSICAL & ENGINEERING SCIENCES

IGURE 1. Typical stationary-crystal photograph of anthrone, 20 °C, showing two types of diffuse spot: [010] vertical, white + Cu K radiations. ([010] left-to-right in figures 1 to 3).

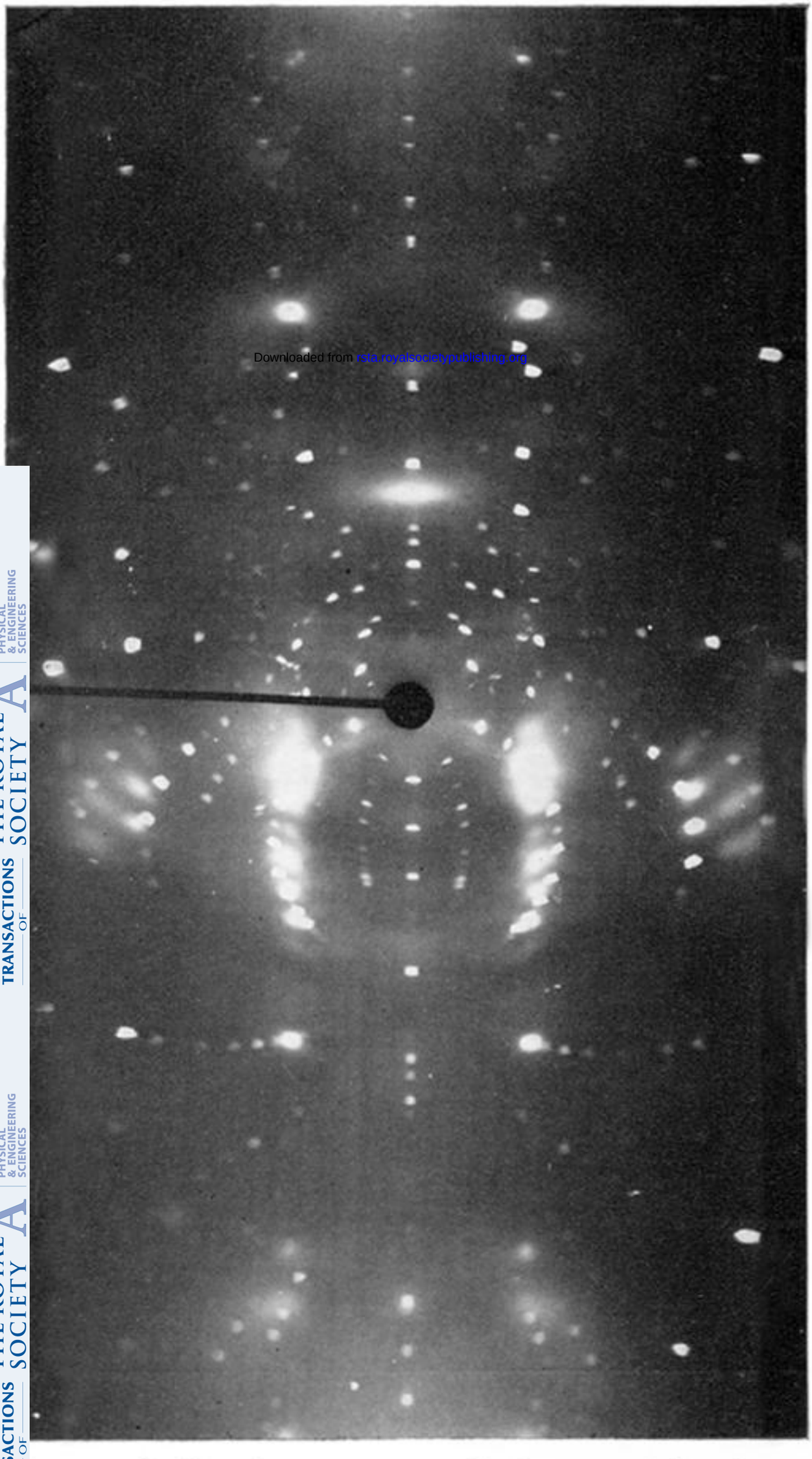

PHILOSOPHICAL TRANSACTIONS OF THE ROYAL SOCIETY A MATHEMATICAL, PHYSICAL & ENGINEERING SCIENCES

IGURE 2. Stationary-crystal photograph of anthraquinone, in a setting near to that of the isostructural anthrone (figure 1). No 'disorder' spots.

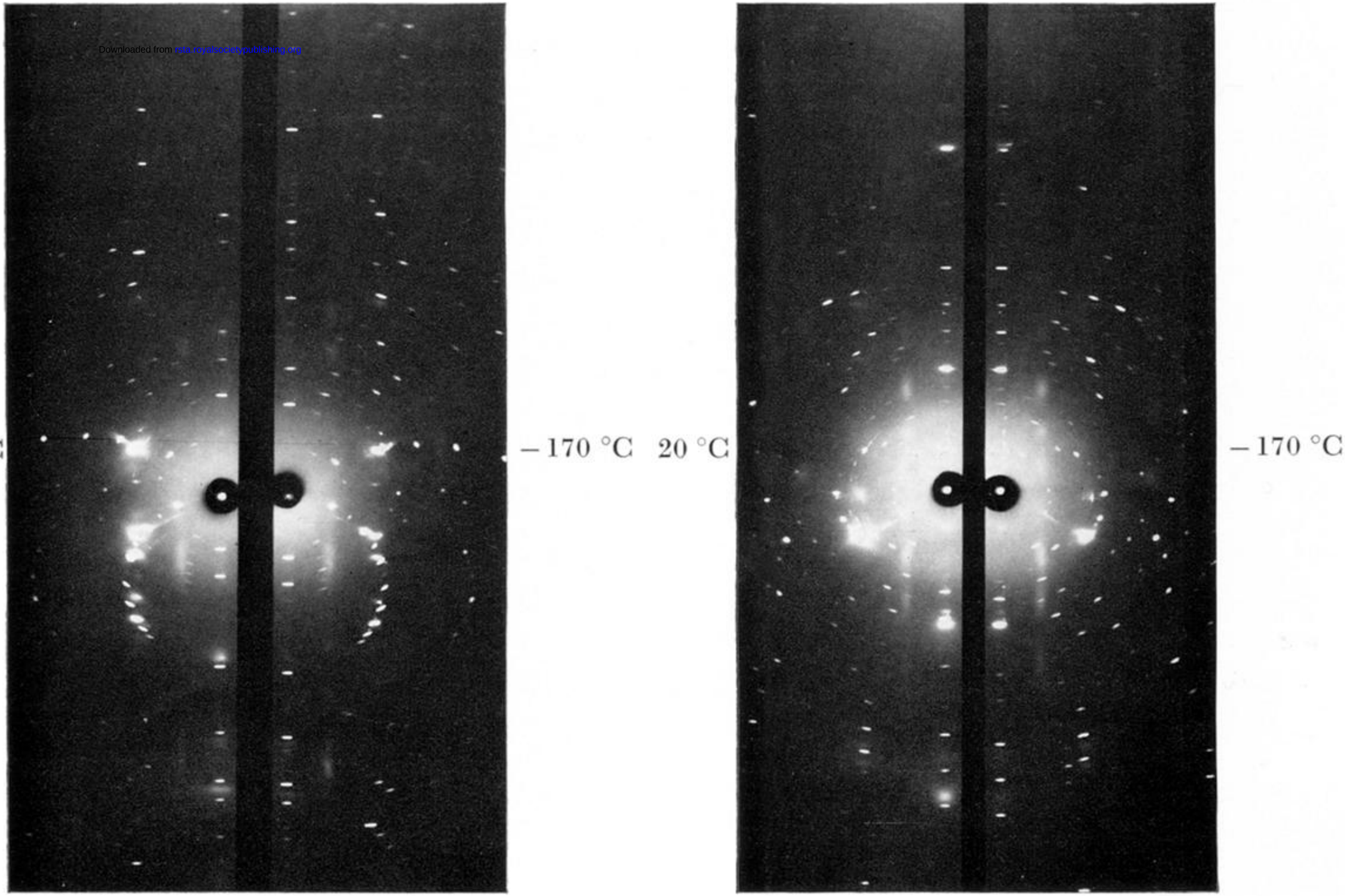

FIGURE 3. A pair of similar anthrone photographs taken at 20 °C (left), and – 170 °C (right) respectively Two different settings. The thermal diffuse scattering is weakened at low temperatures, whereas most Laue spots and the 'disorder' diffuse scattering are relatively more intense.

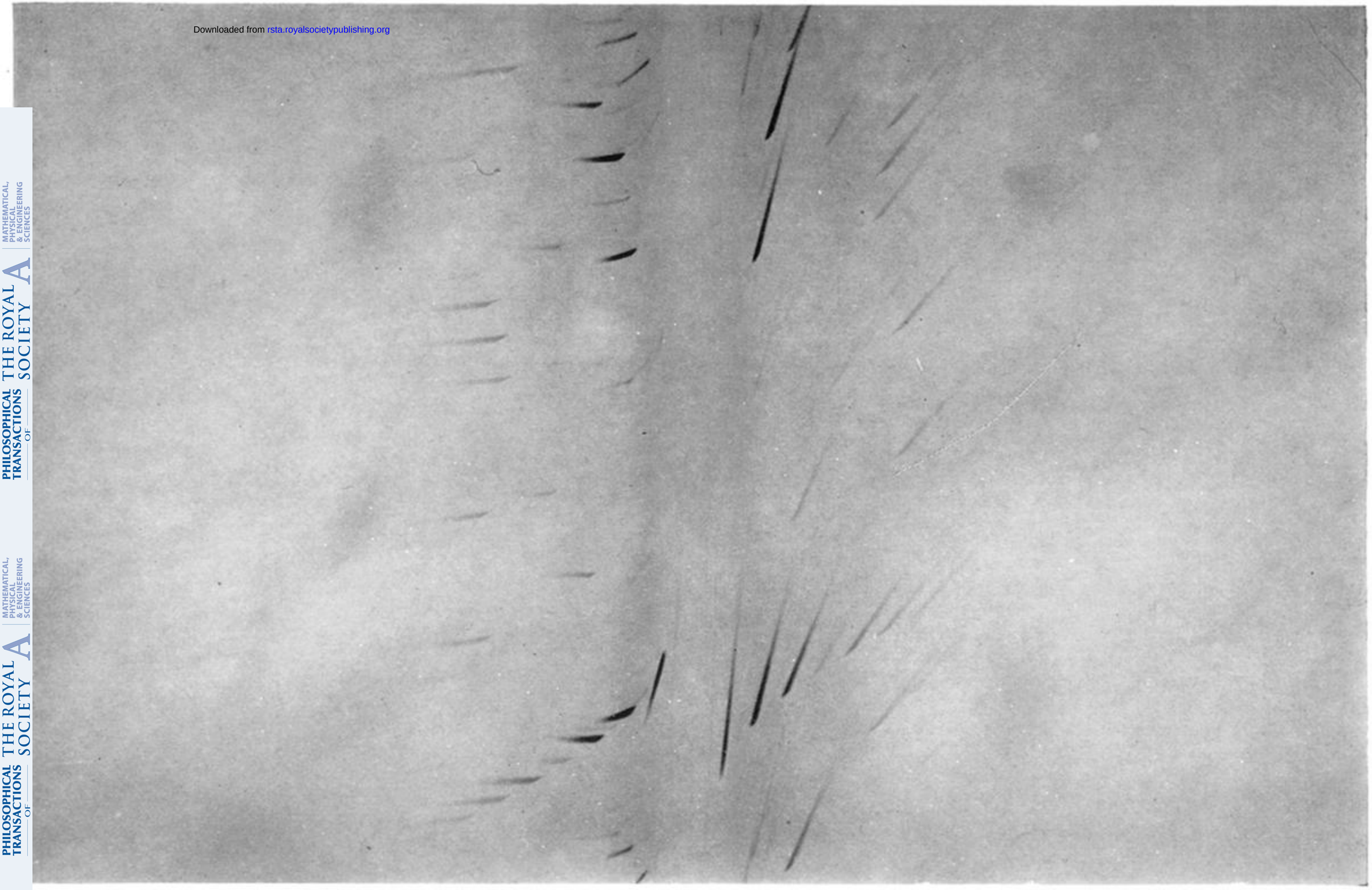

FIGURE 4. Equi-inclination Weissenberg $\{h\ \frac{3}{2}\ l\}$ photograph of anthrone, 48 h exposure time, filtered Cu Kα radiation, 5.73 cm diameter Nonius camera. Note comparative lack of detail.

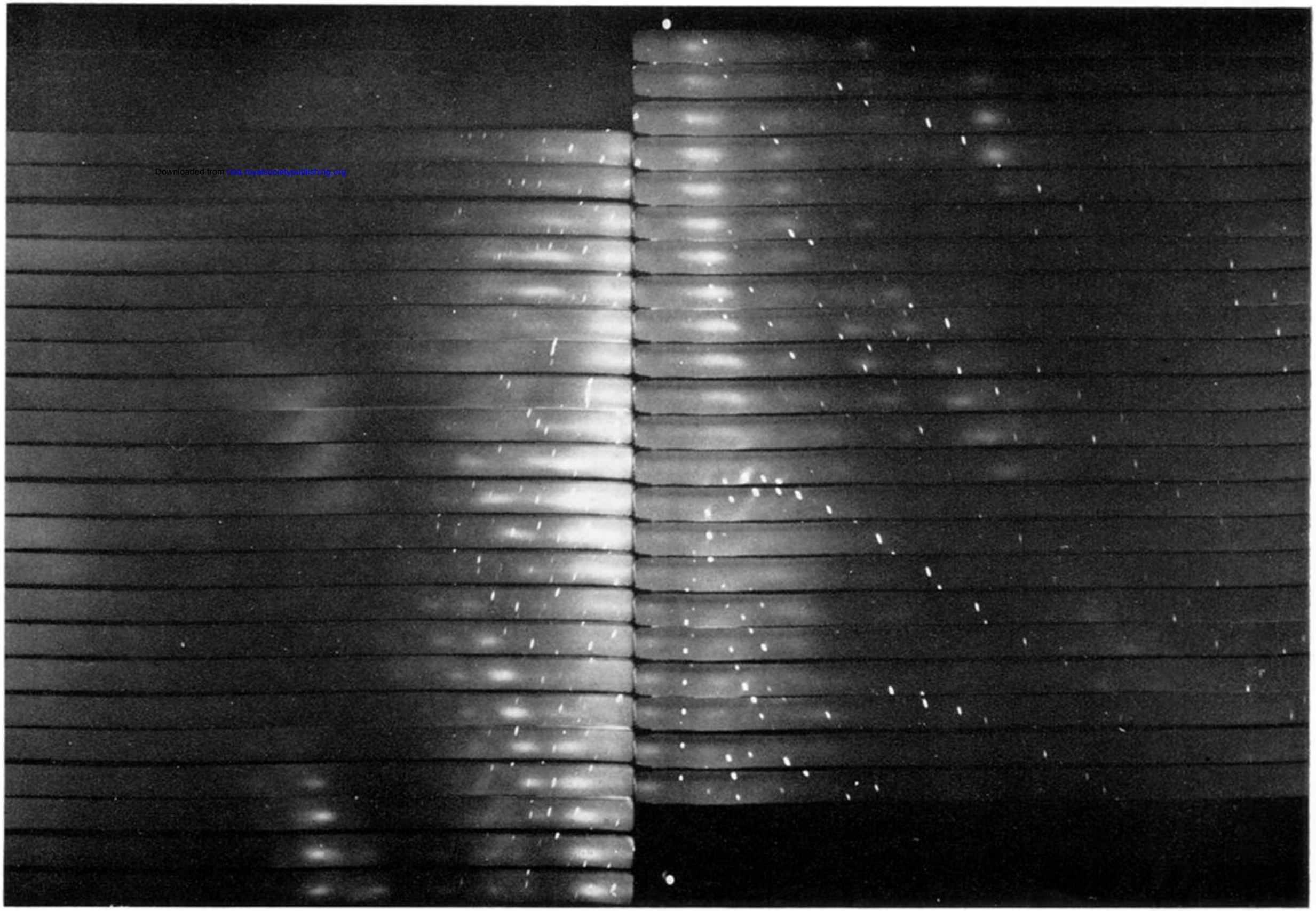

FIGURE 5. One set of $\{h\,\frac{1}{2}\,l\}$ (left) and $\{h\,\frac{3}{2}\,l\}$ (right) stationary-crystal strip photographs taken on a Weissenberg camera set for equi-inclination $\{h\,1\,l\}$. Each of the 22 crystal orientations was given 2 h exposure time before resetting the crystal by 5° at a time and moving the camera forward by a corresponding 2.5 mm. Note the increased intensity and resolution as compared with figure 4. (Figure 5 is at right angles to figures 1, 3, plate 10.)